



LAWRENCE  
LIVERMORE  
NATIONAL  
LABORATORY

# GLOBAL P-WAVE TOMOGRAPHY FOR IMPROVED TRAVEL TIME PREDICTIONS AND EVENT LOCATIONS

N. A. Simmons, S. C. Myers, G. Johannesson, E.  
Matzel

June 29, 2012

The 2012 Monitoring Research Review  
Albuquerque, NM, United States  
September 18, 2012 through September 20, 2012

## **Disclaimer**

---

This document was prepared as an account of work sponsored by an agency of the United States government. Neither the United States government nor Lawrence Livermore National Security, LLC, nor any of their employees makes any warranty, expressed or implied, or assumes any legal liability or responsibility for the accuracy, completeness, or usefulness of any information, apparatus, product, or process disclosed, or represents that its use would not infringe privately owned rights. Reference herein to any specific commercial product, process, or service by trade name, trademark, manufacturer, or otherwise does not necessarily constitute or imply its endorsement, recommendation, or favoring by the United States government or Lawrence Livermore National Security, LLC. The views and opinions of authors expressed herein do not necessarily state or reflect those of the United States government or Lawrence Livermore National Security, LLC, and shall not be used for advertising or product endorsement purposes.

# GLOBAL P-WAVE TOMOGRAPHY FOR IMPROVED TRAVEL TIME PREDICTIONS AND EVENT LOCATIONS

Nathan A. Simmons, Stephen C. Myers, Gardar Johannesson and Eric Matzel

Lawrence Livermore National Laboratory

Sponsored by National Nuclear Security Administration

Contract No. DE-AC52-07NA28539/LL12-SignalPropagation-NDD02

## **ABSTRACT**

We develop a global-scale P-wave velocity model (LLNL-G3Dv3) designed to accurately predict seismic travel times at regional and teleseismic distances simultaneously. The model provides a new image of Earth's deep interior, but the underlying practical purpose of the model is to provide enhanced seismic event location capabilities. Previous versions of LLNL-G3D provide substantial improvements in event location accuracy due to a more explicit Earth representation from the surface to the core and 3-D ray tracing. The latest model is based on ~2.8 million *P* and *P<sub>n</sub>* arrivals that are re-processed using our global multi-event locator known as Bayesloc. We construct LLNL-G3Dv3 within a spherical tessellation based framework, allowing for explicit representation of undulating and discontinuous layers including the crust and transition zone layers. Using a multi-scale inversion technique, regional trends as well as fine details are captured where the data allow. LLNL-G3Dv3 exhibits large-scale structures including cratons and superplumes as well numerous complex details in the upper mantle, including the transition zone. Particularly, the model reveals new details of a vast network of subducted slabs trapped within the transition beneath much of Eurasia, including beneath the Tibetan Plateau. We demonstrate the impact of Bayesloc multiple-event location on the resulting tomographic images through comparison with images produced without the benefit of multiple-event constraints (single-event locations). We find that the multiple-event locations allow for better reconciliation of the large set of direct P phases recorded at 0-97° distance and yield a smoother and more continuous tomographic model than the single-event locations, even when an iterative inversion/relocation technique is employed. We demonstrate that travel time predictions can differ by seconds at regional distances and up to a second at teleseismic distances, depending on the initial locations of the input data. Therefore, accurate locations of the tomographic input data are crucial for developing a model with the ability to accurately locate future events. Event location validation tests with our preferred model (LLNL-G3Dv3) yield epicenter mislocation improvements of 60% using only regional arrivals, 30% improvement using only teleseismic arrivals, and a gradation of improvement between 30% and 60% when regional and teleseismic data are used together. These tests demonstrate the value of global 3-D tomography for predicting future event locations. This work performed under the auspices of the U.S. Department of Energy by Lawrence Livermore National Laboratory under Contract DE-AC52-07NA27344. LLNL-PROC-?

## **OBJECTIVES**

The overall objective of this project is to generate a global-scale 3-D image of the Earth's crust and mantle that is capable of accurately predicting regional and teleseismic travel times. Achieving this objective will allow for accurate seismic event location determination for events occurring anywhere on the globe. The sub-objectives outlined in this report include: 1) the design of a global model of P-wave velocity structure that predicts P and Pn travel times globally, and 2) demonstrating the importance of multiple-event locations for the input data prior to tomographic inversion.

## **RESEARCH ACCOMPLISHED**

We develop a new global P-wave tomography model called LLNL-G3Dv3 by leveraging several imaging techniques outlined in previous Monitoring Research Review proceedings (Simmons et al. 2009, 2010a, 2011a) and journal articles (Myers et al. 2011; Simmons et al. 2011b). The model also leverages starting models including the global joint seismic-geodynamic model called GyPSuM (Simmons et al. 2010) and the Regional Seismic Travel Time (RSTT) model (Myers et al. 2010). We invert travel times for a global distribution of events with locations determined via the Bayesloc multiple-event location technique (Myers et al. 2007, 2009, 2011), modified in the current study to account for regional travel time curve trends. We compare our location procedures and model results to a global model obtained without the benefit of multiple-event location prior to tomographic inversion. Predicted travel times are found to be substantially different depending on the initial locations of events used to develop the image.

### **Dataset and Multiple-event Clustering Technique**

Travel time data were gathered from the Lawrence Livermore National Laboratory (LLNL) database (see Ruppert et al., 2005), which is a massive compilation of data from a variety of sources. Those include the EHB bulletin (Engdahl et al., 1998) provided by the International Seismological Centre (ISC), the National Earthquake Information Center (NEIC) bulletin, and a variety of regional bulletins. Additional data are derived from seismic deployments for Peaceful Nuclear Explosions (PNE's), large refraction surveys, the USARRAY Transportable Array (TA) and temporary PASSCAL deployments around the world. A large number of the travel time measurements were made by staff at LLNL. Currently, the full travel time data consists of ~13.4 million measurements from ~118,000 seismic events.

Given the redundancy of very large tomography data sets, many studies choose to combine the information by forming summary rays through simple averaging or a more sophisticated process. Instead of forming summary rays, we chose to select specific events to be simultaneously relocated with Bayesloc. Therefore, we designed an event selection strategy to find seismic events with the highest probability to be accurately located using the Bayesloc procedures and events that provide the greatest number of P and Pn data for tomography. The selected events include all available Ground Truth level 5 (GT5) or better based on the Bondár et al. (2004) criteria. In addition, we selected events with the most:

- 1) teleseismic P travel time measurements,
- 2) even azimuthal coverage of the teleseismic networks
- 3) regional Pn travel time measurements, and
- 4) local Pg measurements provided that Pn or P measurements exist for the event.

Sampling was achieved by rank-ordering events based on the four criteria. The first event in the list was selected and other events within 1° were removed from consideration for that criterion. Event sampling with the above selection criteria was repeated for events in 6 depth bins: 0-35 km, 35-75 km, 75-150 km, 150-300 km, 300-450 km and 450-700 km depth range.

Through this selection process, we reduced the number of considered events to 13,069 of the global seismic events with the most measurements and the best network geometry. The selected events provided ~3.4

million travel time measurements for a suite of teleseismic, regional, and depth phases (Table 1) recorded at 7,370 seismic stations worldwide.

**Table 1: Travel time arrivals for input into Bayesloc multiple-event location**

Phase	Number	
	Input to Bayesloc	Used in tomography
P	2,662,081	2,553,180
Pn	286,297	266,882
pP	182,890	
Sn	80,912	
sP	78,696	
PcP	62,458	
Pg	30,911	
Lg	22,162	
Total	3,406,407	2,820,062

The 13,069 events were located using the Bayesloc multiple-event location technique (Myers et al. 2007, 2009), previously applied to a global dataset (Myers et al. 2011). Bayesloc is a formulation of the multiple-event location system that includes travel-time corrections, arrival-time measurement (pick) precision, and stochastic phase labels. The hierarchical Bayesian formulation allows for prior constraints on any aspect of the multiple-event system, and a Markov-chain Monte Carlo method is used to draw samples from the joint distribution of multiple-event location parameters.

The Bayesloc travel-time correction formulation includes a correction to the travel time curve for each phase, which accounts for regional travel-time error trends. To the travel time curve corrections, Bayesloc adds station and event terms with a zero-mean prior constraint to account for small, path-dependent errors. Myers et al. (2011) relocated a set of global events, but limited regional-distance travel time data to the Middle East. Therefore, one adjustment for each regional-phase travel time curve was sufficient. In this study we include regional-phase data from all parts of the globe, which necessitates spatially variable corrections to regional-phase travel time curves. Varying regional travel time curve corrections are achieved by forming a cluster of neighboring events around each event and simultaneously relocating the cluster (see Figure 1 for cluster examples). In addition to allowing for region-specific travel-time curve corrections, simultaneous relocation of event clusters maintains the ability to propagate prior constraints from GT0-GT5 through the data set and provides robust estimates of pick precision and phase labels.

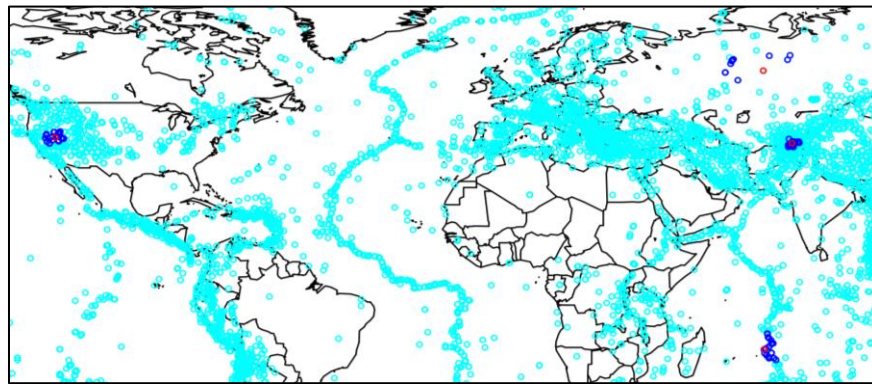


**Figure 1.** Examples of event clusters formed during the Bayesloc multiple-event relocation process. Red circles are the 4 example target events and dark blue circles are events that are members of each cluster. Light blue circles mark events not used to form any of the example clusters.

Bayesloc multiple-event processing results in median epicenter shifts of 6.8 km, depth shifts of 5.5 km, and origin time shifts of -0.67 seconds compared to single-event locations (Figure 2). Figure 2 shows that

epicenter shifts are not random, but rather regionally dependent. The largest shifts are observed at subduction zones, where events tend to move trenchward, which is consistent with the observations and reasoning of Creager and Boyd (1992). Many events in the Former Soviet Union are explosions with known locations and hence display small epicenter shifts, as the locations are constrained by priors. After Bayesloc processing we remove events if the 90% epicenter probability region for that event exceeds 1000 km<sup>2</sup> in area. Events are also removed if the depth uncertainty exceeds 18 km or if the origin time uncertainty exceeds 1 second. Individual travel time picks are removed if the phase label is not determined with probability greater than 0.95 or if arrival-time uncertainty is greater than 1 second. Based on these criteria, the number of events is reduced to 12,571 (3.8% reduction) and the number of P and Pn picks is reduced from 2,948,378 to 2,820,062 (4.3% reduction). Relocation using Bayesloc and removal of a relatively modest percentage of untrusted data results in a reduction in travel time residuals (w.r.t. ak135) from 1.59 seconds to 1.26 seconds, which equates to a 37% reduction in variance.

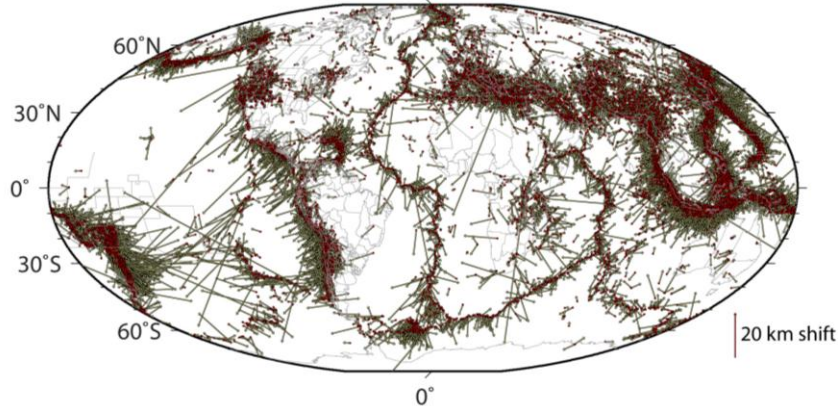


**Figure 2.** Bayesloc multiple-event relocation vectors. The red circles mark the epicenter locations determined one event at a time (single-event locations). Arrows illustrate the epicenter shifts due to multiple-event relocation using the clustering technique described in the text.

### The LLNL-G3Dv3 Model and Location Validation

The LLNL-G3Dv3 model is parameterized with nodes defined by triangular tessellations of spherical surface. Spherical tessellation grids have been employed in numerous global geophysical studies primarily for generating evenly spaced points and avoiding polar distortions created by latitude-longitude grids (e.g. Wang and Dahlen, 1995). Spherical tessellation grids are conveniently extensible to any resolution level and hierarchies of different resolution grids are intrinsic. Within the spherical tessellation framework, we represent undulating and discontinuous layers by placing nodes at arbitrary radii. The maximum lateral resolution considered is  $\sim 1^\circ$  spacing laterally, and 57 layers from the surface to the core (giving  $\sim 1.6$  million points). We exploit the hierarchical nature of the tessellation grid through our multi-resolution inversion approach called Progressive Multi-level Tessellation Inversion (PMTI) developed in Simmons et al. (2011).

The effort to generate complex global-scale tomography models is motivated by the fact that accurate model-based travel time prediction necessitates 3-D ray tracing given significant ray path discrepancies between 1-D and 3-D ray paths. Deviations in the ray paths from the 1-D assumption are particularly large where high degrees of velocity variability exist, such as in the shallow upper mantle where regional rays travel. Thus, we adapted a 3-D ray tracing approach based on the Zhao et al. (1992) methodology. Our particular adaptation of the 3-D ray tracing methodology is described in Simmons et al. (2011).

The PMTI imaging technique yields multi-resolution images without developing irregular grids and also provides intrinsic regularization similar to a regionally variable smoothing operator. The only regularization required to generate reasonable images is a single damping term. We identify the appropriate damping level with basic L-curve analysis (Figure 3). The optimum model (providing a balance of image roughness and data misfit) fits the  $\sim 2.8$  million P-wave arrivals with an overall standard

deviation of 0.96 seconds. This equates to 64% variance reduction relative to the initial event locations and travel time residuals with respect to the ak135 model.

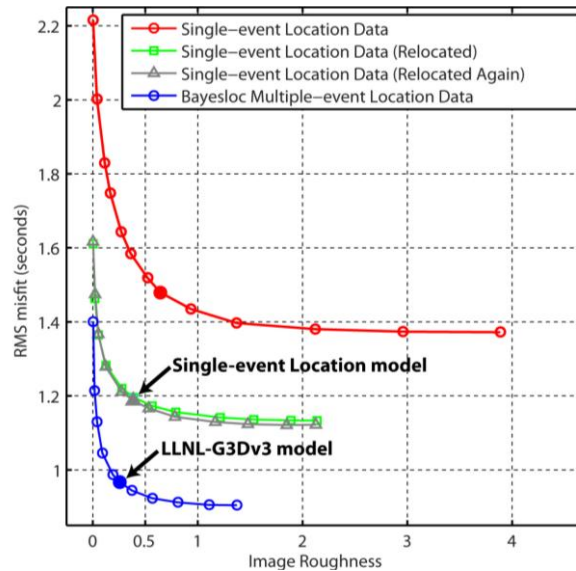


**Figure 3.** Roughness versus data misfit for a spectrum of damping weights. The multiple-event locations allow for higher degrees of data fit relative to single-event locations, even when an iterative tomography/inversion procedure is employed.

Long-wavelength features in the shallow upper mantle are depicted where P-wave coverage is limited, such as beneath ocean basins (Figure 4). As noted in Simmons et al. (2010), joint inversion of multiple data types that include seismic and geodynamic constraints is a powerful way to estimate heterogeneities where single types of data may provide only limited constraints. Specifically to this modeling effort, it is extremely difficult to resolve reasonable images of P-wave velocity heterogeneity associated with mid-ocean ridges and entire cratons without inversions including surface-reflected multiples and/or surface waves. Since our starting model is based on the joint seismic-geodynamic model (GyPSuM), many of the shallow regions with considerable data gaps are filled in with reasonable estimates of velocity heterogeneity. Thus large portions of the velocity anomalies attributed to cratonic roots and linear mid-ocean ridge structures are also seen as dominant structures in the LLNL-G3Dv3 model.

Although many of the long-wavelength shallow upper mantle structures are largely seen in the starting model, details in the shallow upper mantle P-wave velocity structure are better resolved in several regions; particularly where data are abundant such as beneath the North American continent and large portions of Eurasia. Complex velocity structures are clearly evident along tectonic margins, where active seismicity yields numerous data providing powerful constraints. However, we note that complexities in the shallow upper mantle are also found well within the stable continental interiors of North America and Eurasia, where substantial regional travel time data exist as well. These mostly stable cratonic/platform regions are clearly less complex than tectonically active regions and are generally imaged as long-wavelength features. However, stable continental regions may be more complex than generally recognized, due to a lack of resolution.

Like many previous global P-wave tomography studies, we image tabular subducted slabs in the upper mantle along most of the world's active (or recently active) convergent margins and ancient slabs in the lower mantle. We also detect large high-velocity structures within the transition zone beneath much of Eurasia, which are likely subducted slabs deflected horizontally near the 660-km discontinuity and trapped within the transition zone. These trapped slab structures beneath the Eurasian continental interior tend to have sharper velocity gradients along the edges and are more expansive in the LLNL-G3Dv3 model than most global P-wave models

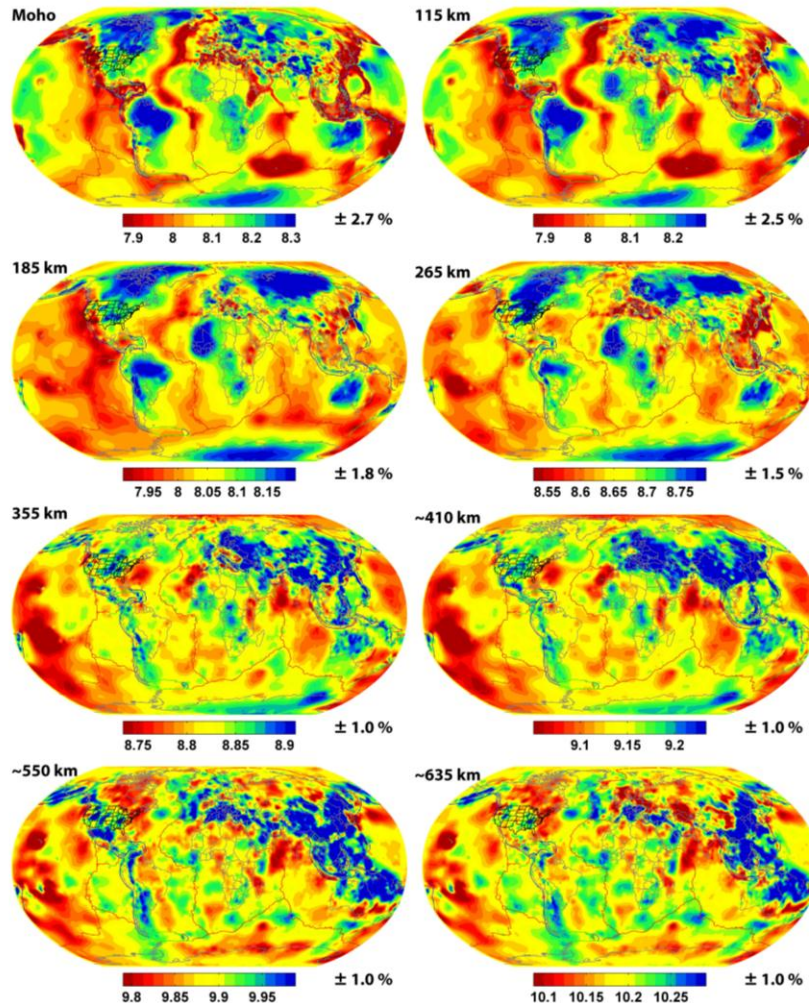


**Figure 4.** The LLNL-G3Dv3 model P-wave velocity structure in the upper mantle.

Along the western Pacific margin, the fast anomalies in the transition zone have long been identified as subducted Pacific lithosphere deflected near the base of the upper mantle. However, we also detect a broad fast anomaly above and within the transition zone beneath western China. The anomaly extends from India to Mongolia and lies directly beneath the Tibetan Plateau (see Figure 4). This broad fast anomaly is possibly a large remnant slab subducted during the convergence of India with Eurasia and thus the closing of the Tethys Oceans. It has proven difficult to identify enough subducted lithosphere in the Tethys region from tomographic images to account for the expected volume of slabs subducted since the Mesozoic Era (Hafkenscheid et al., 2006). It is apparent that substantial quantities of lithosphere has subducted into the lower mantle deep beneath present-day India, contributing to the estimated volumetric budget of subducted material. However, our model indicates that a large volume of the subducted material is trapped in the transition zone beneath most of western China (Figure 4).

Preliminary travel time and location validation tests were performed on a globally distributed set of 116 explosions with known locations and earthquakes with locations constrained by a local network. Validation events were excluded from the tomographic inversion to prevent circularity. Test data sets for each event consisted of a specified number of randomly selected P and Pn arrivals. Ten random realizations were drawn for each test set, unless fewer than ten unique permutations were possible. Each data realization was used to relocate the events and summary statistics were computed for each data category (number of P and Pn data). Based on these preliminary relocation tests, epicenter mislocation errors are generally reduced by

~60% when only regional phases are used, and ~30% when only teleseismic phases are considered (Figure 5). A comprehensive validation study is currently underway and will be the subject of an upcoming report.

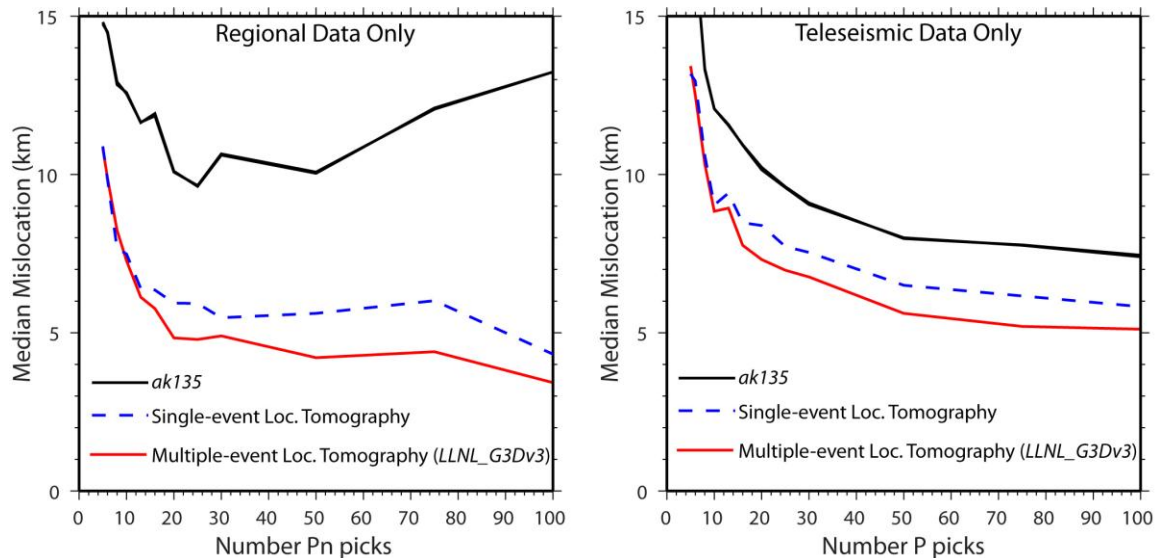


**Figure 5.** Median mislocations for the 116 well-known test events. Independent tests were performed with 3 models: ak135, Single-event location model, and the Multiple-event location model (LLNL-G3Dv3).

### Single-event Locations versus Multiple-event Locations

Knowledge of the location of past seismic events used to develop tomography models is a classical problem, and is of particular importance when designing a model that allows for accurate prediction of future event locations. To test the importance of the multiple-event locations used to develop LLNL-G3Dv3, we developed an alternative model using the common approach of iterative tomography/relocation beginning with event locations determined without the aid of multiple-event constraints. We refer to these alternative event locations as *single-event locations* (or ‘SELs’) since individual events are located independent of the others (a standard global tomography approach). For clarity of further discussion, we will refer to the multiple-event locations as ‘MELs’.

Identical to the procedures described in previous sections, we constructed a roughness versus misfit trade-off curve to estimate the appropriate damping weights (Figure 3). It is immediately evident that the same level of fit obtained using the MELs is impossible to achieve with the SELs. This observation holds even when no damping constraints are used in the tomographic inversion. With a damping weight that balances misfit and image roughness, the root-mean-squared (RMS) misfit of the SELs data is 1.47 seconds compared to 0.96 seconds using the MELs. It should also be noted that the image produced using the SELs data is more than 2 times rougher, suggesting that a much more complex model is required to explain the data when these event locations are assumed.

After generating a tomographic model with the SELs data, we relocated the events in single-event mode using the newly generated tomographic model. We find that the new SELs tend to move in the direction of the MELs. To demonstrate this behavior, we computed the parallel and normal components of SELs relocation vectors relative to the MELs relocation vectors and mapped out the occurrences (Figure 6). If all of the relocated SELs were co-located with the MELs, all events would plot at (1, 0). We find that the mode of the occurrences is at 0.70 in the direction of the MELs and -0.10 normal to the MELs. It is evident from this analysis that the SELs tend to move in direction of the MELs, but there exists a substantial spread in the distribution. With these adjusted SELs, the data fit substantially improves (Figure 3). However, the MELs still provide a better fit to the data, with a less complicated tomographic model.

It may be expected that performing the iterative tomography/relocation procedure again would allow the SELs to eventually converge to the MELs. However, we find no clear indications that we can determine the same event locations with this approach (Figure 6). We also find that a 2<sup>nd</sup> tomography/relocation cycle does not allow for significant improvement in data fit (Figure 3).

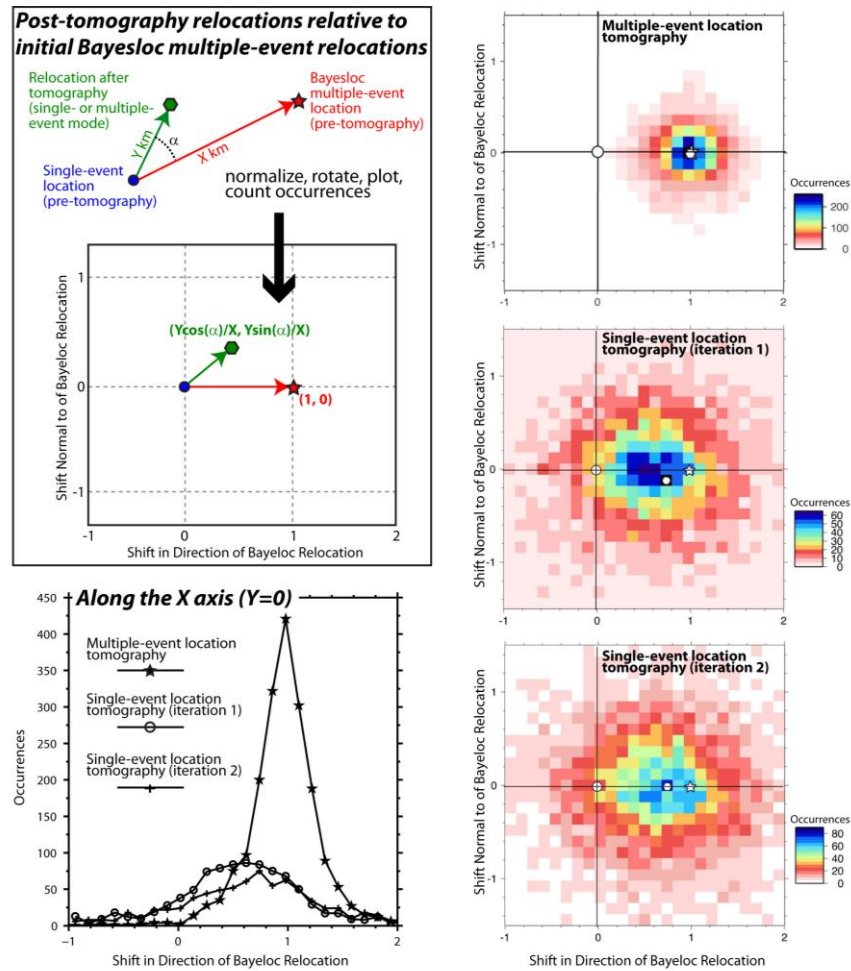


**Figure 6.** Epicenter relocations after tomography compared to initial (pre-tomography) Bayesloc multiple-event locations. Multiple-event locations tend to be stable after tomography, whereas single-event locations tend to shift in the direction of the multiple-event locations (but never converge).

The tomographic image produced with the relocated single-event locations (referred to as the ‘SEL model’) differs from the LLNL-G3Dv3 model produced with multiple-event locations (MELs). The differences are most notable in the shallow upper mantle and transition zone. The differences between the tomographic models often appear localized and subtle, but this is not always the case. For example, the Cocos slab and the deeper Farallon anomaly appear to be a single continuous structure beneath the northern edge of the Caribbean plate in the LLNL-G3Dv3 model (Figure 7). The SEL model depicts a very different configuration. Namely, the Cocos plate appears faster and broader in the shallow mantle and is disconnected from the ancient Farallon remnant in the transition zone and lower mantle. Although it is not known which model most closely resembles the actual Earth, it is clear that the SEL and LLNL-G3Dv3 models are distinctly different.

Although it is not known which model most closely resembles the actual Earth, it is clear that the SEL and LLNL-G3Dv3 models are distinctly different. For the purposes of this study, one of our primary concerns is how each of the models predicts travel times. Therefore, we computed direct P-wave travel times for

each of the 3-D models (SEL and LLNL-G3Dv3 models) to understand how the velocity differences translate to travel time prediction differences. An example travel time grid is shown in Figure 8. Travel time residuals often reach  $\pm 4$  seconds relative to the 1-D ak135 model at regional and intermediate distances (up to  $\sim 23^\circ$  degrees).

The two 3-D velocity models often produce fairly similar travel time residual patterns overall; however, there still are marked differences in the predicted travel times. The differences between the LLNL-G3Dv3 and SEL model travel times often exceed 50% of the difference relative to the ak135 model. More specifically, we find that the differences in travel times predicted by the two 3-D models can be 2 seconds or more at regional/intermediate distances (compared to  $\sim 4$  seconds relative to ak135) and 1 second or more at teleseismic distances (compared to  $\sim 2$  seconds relative to ak135). These residual travel time patterns and intensities are important for location determinations; the fact that the patterns are different suggests that each 3-D model will predict different locations for future seismic events. This assertion is confirmed via location validations tests that show a systematic degradation in location performance using the SEL model (Figure 5).

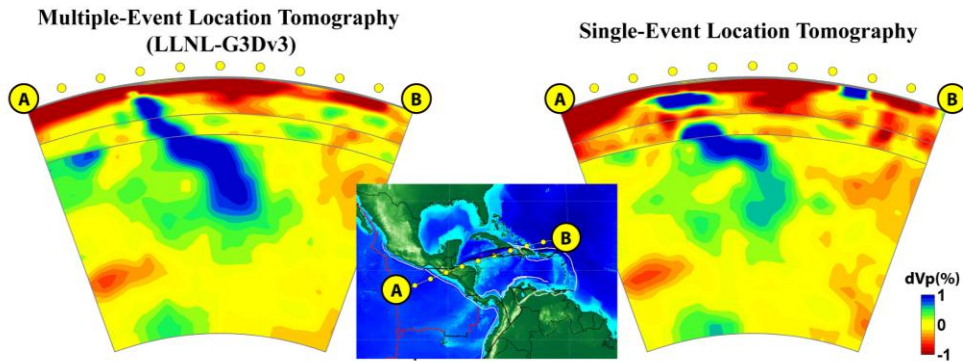


**Figure 7.** Image of the Cocos slab beneath Central America comparing Single- and Multiple-Event location tomography.

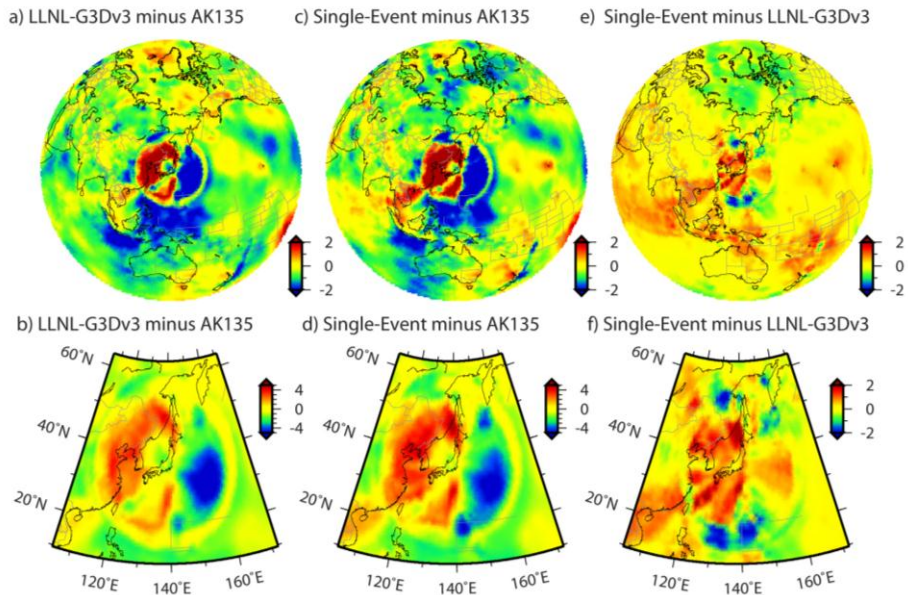


**Figure 8.** Travel time residual patterns for times predicted with LLNL-G3Dv3 and the Single-Event Location model for events up to  $90^\circ$  from station MAJO in Matsushiro, Japan.

## **CONCLUSIONS AND RECOMMENDATIONS**

We have constructed a new global P-wave tomography model called LLNL-G3Dv3 using ~2.8 million P and P<sub>n</sub> travel times and events located with the Bayesloc multiple-event locator, modified for regional travel time curve adjustments. Travel times predicted from the model provide substantial improvement in location accuracy based on some preliminary location validation tests (30-60% mislocation reduction). Comparison of our multiple-event location approach to an iterative tomography/location approach demonstrates that the optimal event locations for the input data may not be realized from the classical iterative approach. We also confirm that the multiple-event locations produce a model that more accurately predicts a globally distributed set of 116 explosions and earthquakes with locations constrained by a local network. We recommend basing a global tomographic with seismic events that are accurately located with a multiple-event location algorithm such as Bayesloc, prior to tomographic inversion.

## **REFERENCES**

- Bondár, I., S. C. Myers, E. R. Engdahl, and E. A. Bergman (2004), Epicenter accuracy based on seismic network criteria, *Geophys. J. Int.*, 156, 483–496, doi:10.1111/j.1365-246X.2004.02070.x.
- Creager, K. C., and T. M. Boyd (1992), Effects of earthquake mislocation on estimates of velocity structure, *Phys. Earth Planet. Inter.*, 75, 63-76, doi:10.1016/0031-9201(92)90118-F.
- Engdahl, E. R., R. van der Hilst and R. Buland (1998), Global teleseismic earthquake relocation with improved travel times and procedures for depth determination, *Bull. Seis. Soc. Amer.*, 88(3), 722-743.
- Hafkenscheid, E., M. J. R. Wortel and W. Spakman (2006), Subduction history of the Tethyan region derived from seismic tomography and tectonic reconstructions, *J. Geophys. Res.*, 111, B08401, doi: 10.1029/2005JB003791.
- Myers, S. C., G. Johannesson and W. Hanley (2007), A Bayesian hierarchical method for multiple-event seismic location, *Geophys. J. Int.*, 171, 1049-1063.
- Myers, S. C., G. Johannesson and W. Hanley (2009), Incorporation of probabilistic seismic phase labels into a Bayesian multiple-event seismic locator, *Geophys. J. Int.*, 177, 193-204.
- Myers, S. C., M. L. Begnaud, S. Ballard, M. E. Pasyanos, W. S. Phillips, A. L. Ramirez, M. S. Antolik, K. D. Hutchenson, J. J. Dwyer, C. A. Rowe and G. S. Wagner (2010a), A crust and upper-mantle model of Eurasia and North Africa for P<sub>n</sub> travel-time calculation, *Bull. Seis. Soc. Amer.*, 100(2), 640-656.
- Myers, S. C., G. Johannesson and N. A. Simmons (2011), Global-scale P-wave tomography optimized for prediction of teleseismic and regional travel times for Middle East events: 1. Data set development, *J. Geophys. Res.*, 116, B04304, doi:10.1029/2010JB007967.
- Ruppert, S., D., Dodge, A. Elliott, M. Ganzberger, T. Hauk and E. Matzel (2005). Enhancing seismic calibration research through software automation and scientific information management, in *Proceedings of the 27th Seismic Research Review: Ground-Based Nuclear Explosion Monitoring Technologies*, LA-UR-05-6407, Vol. 2.
- Simmons, N. A., S. C. Myers and A. Ramirez (2009), Multi-resolution seismic tomography based on a recursive tessellation hierarchy, in *Proceedings of the 2009 Monitoring Research Review: Ground-Based Nuclear Explosion Monitoring Technologies*, LA-UR-09-05276, Vol. 1, pp. 211-220.
- Simmons, N. A., S. C. Myers and G. Johannesson (2010a), Global-scale P-wave tomography designed for accurate prediction of regional and teleseismic travel times for Middle East events, in *Proceedings of the 2010 Monitoring Research Review: Ground-Based Nuclear Explosion Monitoring Technologies*, LA-UR-10-05578, Vol. 1, pp. 211-220.
- Simmons, N. A., A. M. Forte, L. Boschi, and S. P. Grand (2010b), GyPSuM: A joint tomographic model of mantle density and seismic wave speeds, *J. Geophys. Res.*, 115, B12310, doi:10.1029/2010JB007631.
- Simmons, N. A., S. C. Myers ... (2011a), The updated LLNL-G3D global P-wave velocity model and its performance in seismic event location, in *Proceedings of the 2011 Monitoring Research Review: Ground-Based Nuclear Explosion Monitoring Technologies*, LA-UR-11-04823, Vol. 1, pp 188-197.
- Simmons, N. A., S. C. Myers and G. Johannesson (2011b), Global-scale P-wave tomography optimized for prediction of teleseismic and regional travel times for Middle East events: 2. Tomographic inversion, *J. Geophys. Res.*, 116, B04305, doi:10.1029/2010JB007969.
- Wang, Z. and F. A. Dahlen (1995), Spherical-spline parameterization of three-dimensional Earth models, *Geophys. Res. Lett.*, 22(22), 3099-3102.
- Zhao, D., A. Hasegawa, and S. Horiuchi (1992), Tomographic imaging of P and S wave velocity structure beneath northeastern Japan, *J. Geophys. Res.*, 97, 19909–19928.